Inorganic Chemistry

Article

pubs.acs.org/IC

Design and Characterization of Phosphine Iron Hydrides: Toward Hydrogen-Producing Catalysts

Katharina Weber, Thomas Weyhermüller, Eckhard Bill, Özlen F. Erdem,* and Wolfgang Lubitz*

Max Planck Institute for Chemical Energy Conversion, Stiftstrasse 34-36, D-45470 Mülheim an der Ruhr, Germany

Supporting Information

ABSTRACT: Diamagnetic iron chloro compounds [($P^{Ph}_2N^{Ph}_2$)FeCp*Cl] [**1Cl**] and [($P^{Cy}_2N^{Ph}_2$)FeCp*Cl] [**2Cl**] and the corresponding hydrido complexes [($P^{Ph}_2N^{Ph}_2$)-FeCp*H] [**1H**] and [($P^{Cy}_2N^{Ph}_2$)FeCp*H] [**2H**] have been synthesized and characterized by NMR spectroscopy, electrochemical studies, electronic absorption, and ^{57}Fe Mössbauer spectroscopy ($P^{Ph}_2N^{Ph}_2$ = 1,3,5,7-tetraphenyl-1,5-diphospha-3,7-diazacyclooctane, $P^{Cy}_2N^{Ph}_2$ = 1,5-dicyclohexyl-3,7-diphenyl-1,5-diphospha-3,7-diazacyclooctane, Cp* = pentamethylcyclopentadienyl). Molecular structures of [**2Cl**], [**1H**], and [**2H**], derived from single-crystal X-ray diffraction, revealed that these compounds have a typical piano-stool geometry. The results show that the electronic properties of the hydrido complexes are strongly influenced by the substituents at the phosphorus donor atoms of the $P^{R}_2N^{Ph}_2$ ligand, whereas those of the chloro complexes are less affected. These results illustrate that the hydride is a strong-field ligand, as compared to chloride, and thus leads to a significant degree of covalent character of the iron hydride bonds. This is important in the context of possible catalytic intermediates of iron hydrido species, as proposed for the catalytic cycle of [FeFe] hydrogenases and other synthetic catalysts. Both hydrido compounds [**1H**] and [**2H**] show enhanced catalytic currents in cyclic voltammetry upon addition of the strong acid trifluoromethanesulfonimide [$NHTf_2$] (pK_a^{MeCN} = 1.0). In contrast to the related complex [($P^{tBu}N^{Bn}$)$_2$FeCp^{C6F5}H], which was reported by Liu et al. (*Nat. Chem.* **2013**, *5*, 228−233) to be an electrocatalyst for hydrogen splitting, the here presented hydride complexes [**1H**] and [**2H**] show the tendency for electrocatalytic hydrogen production. Hence, the catalytic direction of this class of monoiron compounds can be reversed by specific ligand modifications.

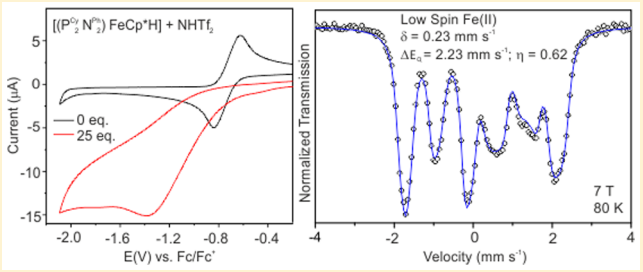

INTRODUCTION

[NiFe] and [FeFe] hydrogenases belong to a class of metalloenzymes that catalyze reversible proton reduction to dihydrogen in biological energy metabolism.[1] [FeFe] hydrogenases predominantly function as catalysts for hydrogen production and generally exhibit higher activity than that of [NiFe] hydrogenases. The active site of [FeFe] hydrogenases consists of a [4Fe−4S] cluster that is attached via a cysteinyl sulfur atom to an [2Fe] subcluster. Both metal ions of the [2Fe] subcluster are coordinated by CO and CN^- ligands and bridged by an azadithiolate ligand.[2−4] Biophysical[3] and theoretical[5,6] studies strongly suggest that an intermediate with a terminal hydride, bound to the distal iron, is involved in the catalytic cycle of [FeFe] hydrogenases. Catalytic steps of hydrogen formation are proposed to occur at the iron center distal to the [4Fe−4S] cluster, and the azadithiolate bridge relays protons to and from the distal iron during catalysis.[4,7]

Modeling the active sites of hydrogenases is a helpful tool in the development process of future artificial catalysts for electrochemical hydrogen production based on abundant inexpensive metals like iron.[8−10] A broad range of structural and functional dinuclear [FeFe] model complexes has been reported in the literature.[11] However, the formation of thermodynamically favored and less reactive bridging hydrides is one of the major problems that leads to a decrease in the activity of dinuclear [FeFe] mimics.[12]

The potential occurrence of bridging hydrido intermediates can be avoided by using mononuclear complexes. Indeed, Felton et al.[13] reported that molecular hydrogen generation from an acetic acid/acetonitrile solution was efficiently catalyzed by the monomeric hydrido complex [$CpFe(CO)_2H$] generated *in situ* from [$CpFe(CO)_2]_2$. The catalytic activity can be additionally improved by the introduction of a pendant base into the coordination sphere of iron. Ott and co-workers developed a series of coordinatively unsaturated pentacoordinate iron compounds bearing amine functions in the second coordination sphere that are active for electrocatalytic hydrogen production with turnover rates of up to 500 s^{-1} from acetic acid solutions.[14−16] The authors came to the conclusion that the free coordination site in these compounds is important for the formation of hydrido intermediates in the catalytic cycle, as demonstrated by DFT calculations. Recent work by Bullock, DuBois, and co-workers shows that monoiron complexes with pendant bases are also suitable electrocatalysts for hydrogen splitting (TOF = 2.1 s^{-1} under 1.0 atm H_2 in the presence of *N*-methylpyrrolidine), with iron hydrides involved in the

Received: April 24, 2015
Published: July 1, 2015

DOI: 10.1021/acs.inorgchem.5b00911
Inorg. Chem. 2015, 54, 6928−6937

Scheme 1. Synthesis of (a) Chlorido Compounds [1Cl] and [2Cl] and (b) Hydrido Compounds [1H] and [2H]

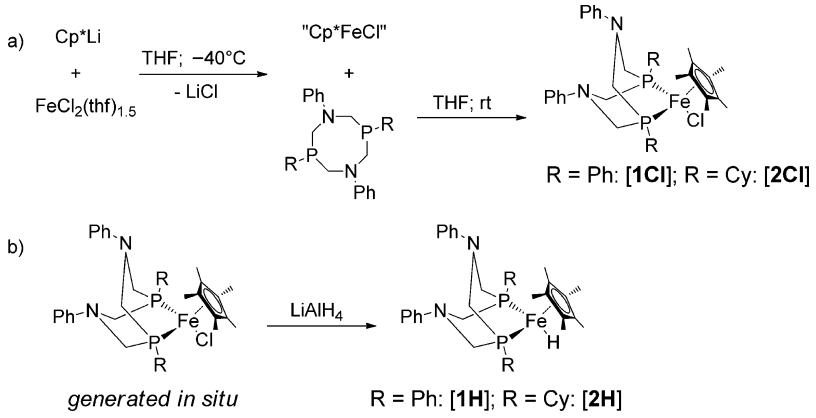

mechanism.[17,18] The postulated heterolytic cleavage mechanism of hydrogen was supported by neutron diffraction analysis of the complex $[Cp^{C_5F_4N}FeH(P^{tBu}{}_2N^{tBu}{}_2H)]^+$, which revealed a strong Fe−H···H−N dihydrogen bond.[19]

Apart from hydrogen conversion catalysis, iron hydrido complexes are fundamentally important for their crucial role in a wide variety of other catalytic processes such as hydrogenation, hydrosilylation, hydroboration, and C−C bond formation.[20] Therefore, a detailed analysis of the electronic structure of well-characterized iron hydrides is of particular interest for a rational design of future catalysts.[21]

In this work, we report synthesis and characterization of a series of $[(P^R{}_2N^{Ph}{}_2)FeCp^*X]$ complexes ($Cp^* = C_5Me_5$, R = cyclohexyl Cy, phenyl Ph, X = Cl, H) with pendant amine bases in the second coordination sphere of iron. A direct comparison of the chloro and the analogous hydrido compounds provides information on the degree of covalency in hydride complexes. Variation of the phosphine substituents (cyclohexyl vs phenyl) and therewith the variation of the electron-donor capability of the ligand allows the electronic structure of the metal center to be fine-tuned.

RESULTS

Synthesis. Chloro complexes [**1Cl**] and [**2Cl**] were synthesized by reaction of Cp*FeCl, prepared *in situ* from Cp*Li and $FeCl_2(thf)_{1.5}$, with the corresponding cyclic 1,5-diphospha-3,7-diazacyclooctane ligand ($P^{Ph}{}_2N^{Ph}{}_2$ in [**1Cl**] and $P^{Cy}{}_2N^{Ph}{}_2$ in [**2Cl**]) in THF solution under an inert atmosphere (Scheme 1a). The isolated solids are stable at room temperature under an inert atmosphere. Both chloro compounds were characterized by ^1H, $^{13}C\{^1H\}$, and $^{31}P\{^1H\}$ NMR spectroscopy (see Experimental Section).

Corresponding hydrido complexes [**1H**] and [**2H**] were synthesized by a reaction of the *in situ* prepared chloro complexes [**1Cl**] and [**2Cl**] with 2.2 equiv of $LiAlH_4$ in THF solution (Scheme 1b). The products are well-soluble in *n*-hexane, Et_2O, and THF but are insoluble in acetonitrile and unstable in chlorinated solvents.

All four compounds show well-resolved ^1H NMR spectra in solution, indicating the presence of diamagnetic Fe(II) low-spin centers. The spectra of [**1H**] and [**2H**] are characterized by triplets at around −16 ppm with $^2J_{PH}$ couplings of ≈60 Hz that are typical for terminal iron hydrides.[17,18,20c,22] The more σ-electron-donating cyclohexyl substituents on phosphorus yield a more upfield-shifted triplet in complex [**2H**] compared to that in [**1H**] (Figure 1). Higher synthetic yields were observed

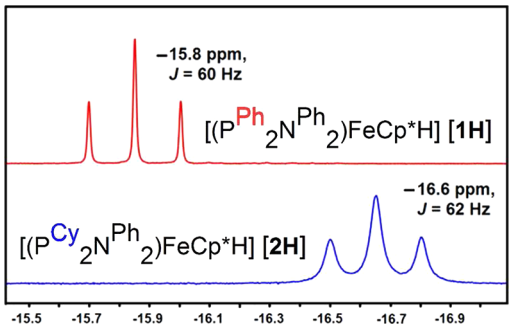

Figure 1. ^1H NMR spectra recorded in C_6D_6 of [**1H**] and [**2H**] showing the hydride region. Full spectra are shown in Figure S1a,b.

when isolated chloro complexes were used as starting material (see Experimental Section). However, this effect is compensated by the fact that one step less is used in the *in situ* preparation pathway. This procedure therefore provides easy and fast access to the hydrido compounds.

Crystallographic Characterization. Single crystals of compounds [**1H**], [**2H**], and [**2Cl**] suitable for X-ray crystallographic analysis could be obtained. Crystallographic details are listed in Table S1 in the Supporting Information, and selected bond distances and angles are given in Table 1.

Molecular structures shown in Figure 2 reveal the typical piano-stool geometry for all three complexes. A comparison of hydrido complexes [**1H**] and [**2H**] shows that the Fe−H bond is affected by the variation of the substituent on phosphorus. In compound [**2H**], containing the more σ-electron-donating cyclohexyl substituent on phosphorus, a longer Fe−H distance (1.59(4) Å), compared to that in phenyl-substituted complex [**1H**] (1.45(2) Å), is observed. However, we are aware that discussion of hydrogen−element bond distances derived from X-ray diffraction data is delicate because the difference in the Fe−H bond lengths might be not as large as the structural analysis indicates (Table 1). A comparison of molecular structures of cyclohexyl-substituted complexes [**2H**] and [**2Cl**] reveals that all iron−ligand distances are longer in the chlorido complex as a consequence of the overall less covalent bonding character in [**2Cl**].

^{57}Fe Mössbauer Spectroscopy. All four complexes were studied by Mössbauer spectroscopy in the solid state at 80 K; experimental parameters together with theoretical values derived from DFT calculations are listed in Table 2. Spectra recorded without applied field (Figures 3 and S3) show well-resolved quadrupole doublets with moderately large quadrupole

DOI: 10.1021/acs.inorgchem.5b00911
Inorg. Chem. 2015, 54, 6928−6937

Table 1. Selected Bond Distances (Å) and Angles in [1H], [2H], and [2Cl] Obtained from X-ray Crystallography and from Optimized Structures (BP86/RI)

	[1H], exp	[1H], calcd	[2H], exp	[2H], calcd	[2Cl], exp	[2Cl], calcd
Fe–X (X = H, Cl)	1.45(2)	1.51	1.59(4)	1.52	2.3436(4)	2.346
Fe–P1	2.1062(6)	2.125	2.1237(7)	2.138	2.1722(4)	2.174
Fe–P2	2.1194(6)	2.124	2.1142(8)	2.137	2.1881(4)	2.175
Fe–Cp* (centroid)	1.718	1.726	1.715	1.728	1.732	1.745
P1–Fe–P2	82.0°	82.4°	81.7°	81.5°	81.1°	80.6°
P1–Fe–X (X = H, Cl)	86.3°	84.6°	91.3°	86.5°	91.5°	90.8°
P2–Fe–X (X = H, Cl)	86.0°	84.7°	91.3°	84.8°	91.5°	91.3°

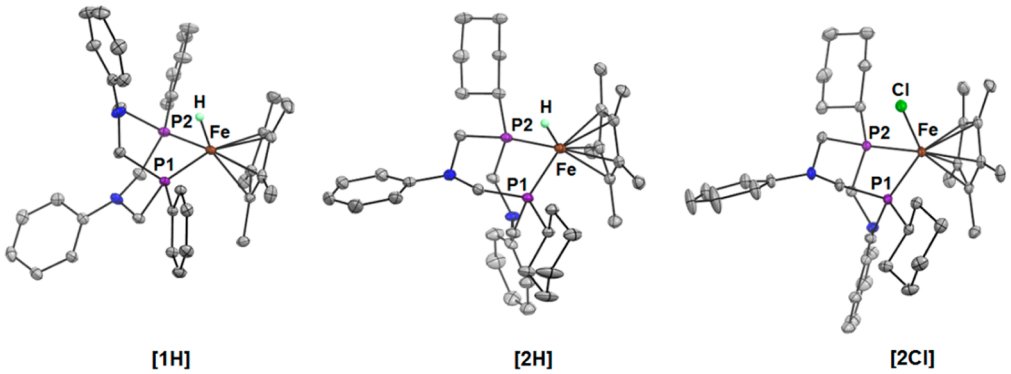

Figure 2. Molecular structures of compounds [1H], [2H], and [2Cl]. Thermal ellipsoids are shown at the 50% probability level. Carbon labels and hydrogen atoms, except hydrides, are omitted for clarity.

Table 2. Experimental (Zero Field, 80 K) and Calculated (B3LYP/CP(PPP)) Mössbauer Parameters

parameter	[1Cl], exp	[1Cl], calcd	[1H], exp	[1H], calcd	[2Cl], exp	[2Cl], calcd	[2H], exp	[2H], calcd
δ [mm/s]	0.46	0.43	0.20	0.18	0.46	0.43	0.23	0.23
ΔE_Q [mm/s]	2.23	2.40	2.11	2.59	2.14	2.49	2.23	2.39
η	0.43	0.38	0.60	0.74	0.38	0.46	0.62	0.35

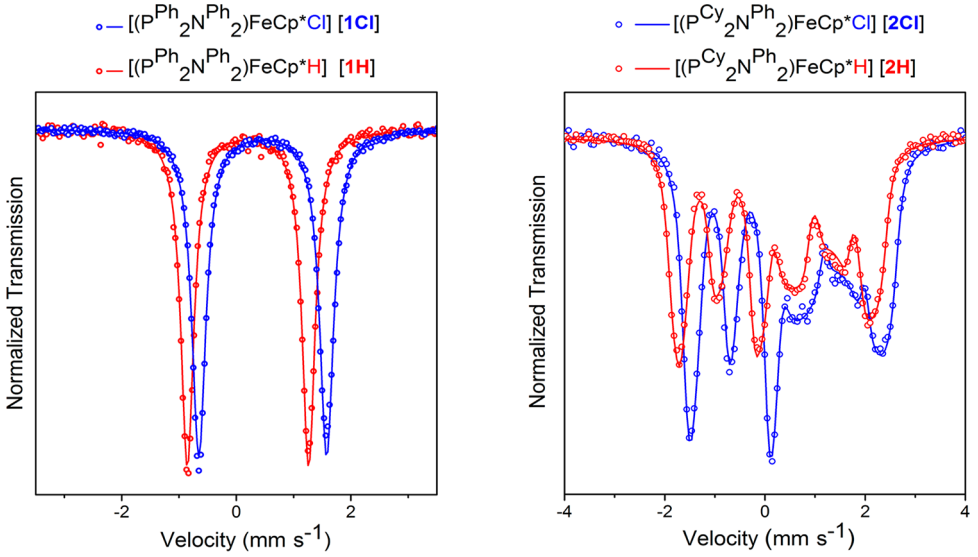

Figure 3. Mössbauer spectra recorded at zero field and 80 K (for [1Cl] and [1H], left) and 7.0 T at 80 K (for [2Cl] and [2H], right). Circles stand for the experimental data, and solid lines stand for the corresponding simulations. Complete sets of the Mössbauer spectra at zero field and 7.0 T for all four compounds and corresponding simulations are shown in Figures S3–S7.

splittings (ΔE_Q = 2.11–2.23 mm/s). The isomer shifts of δ = 0.46 mm/s observed for chloro complexes [1Cl] and [2Cl] and 0.20 and 0.23 mm/s for hydrido complexes [1H] and [2H] are small and lie in the typical range of Fe(II) low-spin complexes. In contrast, the values expected for six-coordinate high-spin Fe(II) would have been typically around 1 mm/s or higher.[23] The differences of 0.26 and 0.23 mm/s in the experimental isomer shifts of the corresponding chloro and hydrido complexes [1H]/[1Cl] and [2H]/[2Cl], respectively, are remarkable and in agreement with the distinct differences in

DOI: 10.1021/acs.inorgchem.5b00911
Inorg. Chem. 2015, 54, 6928–6937

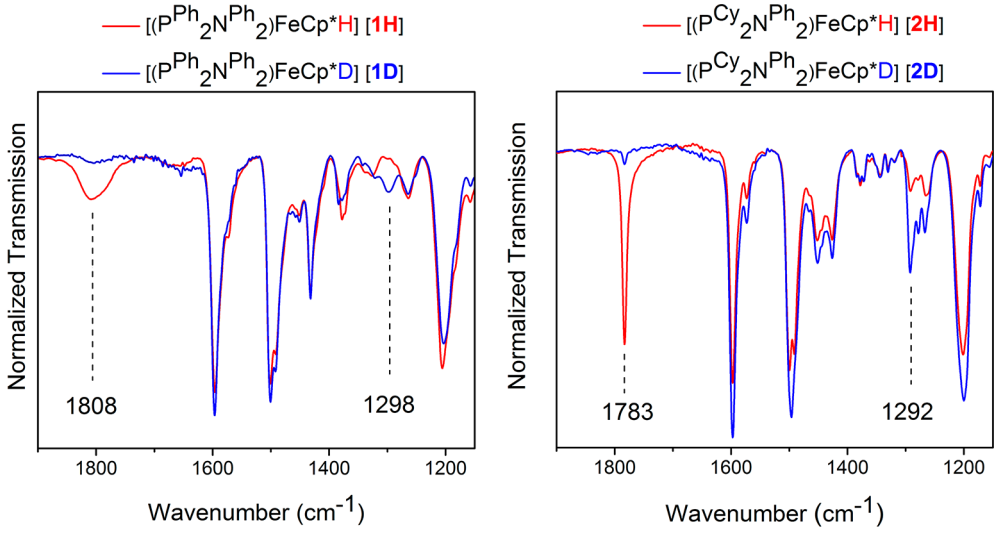

Figure 4. FTIR spectra of [**1H**], [**1D**], [**2H**], and [**2D**] recorded in KBr pellets.

Fe−H and Fe−Cl bond distances observed in the molecular structures of [**2H**] and [**2Cl**]. The shorter Fe−H bonds afford, among other effects, stronger participation of the valence 4s orbital of iron in bond formation, which leads to an increase of s-electron density at the iron nucleus via electron donation from the ligands and, hence, lower isomer shift.[24] The actual differences $|\Delta\delta| > 0.20$ mm/s between the hydride and the corresponding chloride complex are large in view of the fully conserved structure of the other ligands and exceed the variations caused by a change in the oxidation state for Fe(II)/Fe(III) low-spin complexes in other cases.[24] The difference is even larger than that for X = CO and X = H_2O in the series $[FeX(CN)_5]^{3-}$ ($|\Delta\delta| = 0.16$ mm/s)[24] and demonstrates that the hydride ligand is a typical strong-field ligand that forms highly covalent (soft) bonds. This interpretation was confirmed by DFT calculations: while identical δ shifts are predicted for chlorides [**1Cl**] and [**2Cl**], the correct lower isomer shifts are found for [**1H**] and [**2H**]. Moreover, the small difference in δ between hydride complexes [**1H**] and [**2H**] appears to be consistent with the shorter Fe−H bond length in [**1H**] compared to that in [**2H**], using the same argument as above regarding the influence of bond lengths and covalency on the Mössbauer isomer shift, but the bond differences seem to be less dramatic than that indicated by the structural data. Nevertheless, the influence of phosphine substitution on the electronic structure at the iron core is reflected in the overall change in both the isomer shift and the quadrupole splitting for [**1H**] and [**2H**] (Table 2).

The large quadrupole splitting ($\Delta E_Q = 2.11-2.23$ mm/s) of all four compounds reveals significant charge anisotropy in the valence shell of iron. Since the low-spin $3d^6$ configuration of Fe(II) (representing a half-shell) in a crystal field picture has no valence contribution to the electric field gradient (EFG), the large quadrupole splitting is entirely induced by differences in the covalent bonds of the distorted pseudotetrahedral (but, rather, six-coordinate) geometries of these compounds. Therefore, it was not expected that the Cl^-/H^- exchange of weak/strong ligands would yield essentially the same quadrupole splittings. Moreover, magnetically perturbed spectra show that there is no change in the sign of the EFG and only moderate variation in the asymmetry parameter η. DFT calculations, however, which nicely reproduced the ΔE_Q values, finally reveal a significant rotation of the EFG in the molecular frame upon Cl^-/H^- exchange. This phenomenon can be understood as an effect of charge rearrangement, which is seen in the DFT analyses (see Figure S2).

FTIR Spectroscopy. FTIR spectroscopy is a helpful tool for the investigation of transition metal complexes containing terminal hydride ligands. M−H stretching vibrations (ν_{MH}) are observed in the characteristic range of 2200−1600 cm^{-1}.[25,26] Deformational vibrations (δ_{MH}) are not characteristic since they are mixed with other modes of the ligands in the range from 800 to 600 cm^{-1} and are therefore not discussed in this context.

FTIR spectra of [**1H**] and [**2H**] were recorded in the solid state in KBr pellets (Figure 4). A band corresponding to the Fe−H stretching vibration was identified for both [**1H**] and [**2H**] via H/D exchange. The decrease of the vibration energy (in wavenumbers) upon isotopic substitution for both complexes amounts to nearly a factor of $\sqrt{2}$, as predicted by Hooke's law for a diatomic harmonic oscillator. In the FTIR spectrum of phenyl-substituted hydride [**1H**], a broad band at 1808 cm^{-1} is assigned to the Fe−H stretching vibration. Thus, the more covalently bound hydride exhibits a much broader vibrational band. The analogous band in the spectrum of cyclohexyl-substituted [**2H**] is a sharp peak at 1783 cm^{-1}. In agreement with the Mössbauer results discussed above, the lower energy in [**2H**] is an indication of a weaker and less covalent Fe−H bond and a more hydridic hydride. In *n*-hexane solution, broad Fe−H bands at slightly shifted wavenumbers were observed for both hydride complexes (Table 3 and Figure S8).

Electronic Absorption Spectroscopy. The electronic absorption spectra of the iron complexes were recorded in THF

Table 3. FTIR Data of the Fe−H Vibrations in [1H] and [2H] Recorded in KBr Pellets and in Solution[a]

parameter	[1H], solid[b]	[1H], solution[c]	[1H], calcd	[2H], solid[b]	[2H], solution[c]	[2H], calcd
ν_{FeH} [cm^{-1}]	1808	1802	1911	1783	1778	1867
$\delta\nu_{FeH}$ [cm^{-1}]	57	40		12	25	

[a]The calculated values were derived from optimized structures without using a calibration factor. [b]Recorded in KBr pellets. [c]Recorded in *n*-hexane solution; spectra are shown in Figure S8.

DOI: 10.1021/acs.inorgchem.5b00911
Inorg. Chem. 2015, 54, 6928−6937

solution; the respective data are given in Table 4. All four compounds exhibit strong absorption in the UV and blue region due to charge transfer, which, however, is not resolved in well-defined bands. Absorption maxima corresponding to spin-forbidden d−d transitions are resolved at low concentrations, as shown in Figure 5. Note that the corresponding extinction coefficients might have been enhanced due to mixing with charge transfer transitions. Both chlorido compounds reveal three transitions in the region between 26 000 and 14 000 cm^{-1}, whereas both hydride complexes show only one band at around 25 000 cm^{-1}. Optical absorption spectra of transition metal complexes are related to transitions that depend on the ligand field splitting of ground and excited states. Chloride is considered to be a weak π-base, which causes weak ligand field splitting, whereas hydride is among the strongest σ-donating ligands in the spectrochemical series, which leads to large ligand field splitting.[27] Thus, low-energy transitions are observed for the chlorido complexes, and none are observed for the hydrides. Following this simple qualitative analysis of the absorption spectra, we can again deduce that the Fe−H bond is stronger and therefore more covalent in phenyl-substituted compound [**1H**] (ν = 25 773 cm^{-1}) compared to that in cyclohexyl-substituted complex [**2H**] (ν = 24 570 cm^{-1}).

Table 4. Electronic Absorption Maxima Observed for [1H], [2H], [1Cl], and [2Cl] in THF at Room Temperature

compound	wavenumber [cm^{-1}]	wavelength [nm]	extinction coefficient [mM^{-1} cm^{-1}]
[**1H**]	25 773	388	1.74
[**2H**]	24 570	407	1.13
[**1Cl**]	24 813	403	0.99
	20 040	499	0.67
	15 902	629	0.35
[**2Cl**]	25 125	398	0.33
	20 618	485	0.88
	16 426	609	0.24

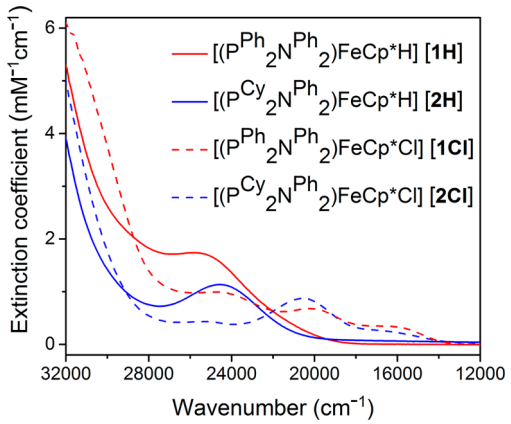

Figure 5. Absorption spectra recorded in THF solutions at 0.0625 mM.

On the basis of all of the crystallographic and spectroscopic (Mössbauer, FTIR, and electronic absorption) results shown above, it is clear that the less electron-donating phenyl-substituent on phosphorus in [**1H**] leads to a more covalent Fe−H bond and thus less hydridic hydride compared to that in compound [**2H**], which carries the stronger σ-donating cyclohexyl-residue on the phosphine ligand.

Electrochemical Characterization. Electrochemical properties of the reported complexes have been investigated using cyclic voltammetry in fluorobenzene solution (1 mM) at a scan rate of 100 mV/s with NBu_4PF_6 (0.2 M) as the supporting electrolyte (Figure 6). Both chlorido compounds show, in solution, reversible oxidation with very similar potentials at −0.67 V for [**1Cl**] and −0.68 V vs Fc/Fc^+ for [**2Cl**] (ΔE_p = 120 mV, $i_{pa}/i_{pc} \approx 1$).[28] The almost identical redox potentials indicate that the change of the substituent on phosphorus does not have a significant impact on the redox behavior of the chlorido complexes. Similar redox potentials were reported for analogous monoiron compounds and were assigned to the Fe(II)/Fe(III) redox couple.[17,18,23,29]

Reversible Fe(II)/Fe(III) redox waves are also observed for the hydride compounds with somewhat shifted potentials at −0.66 V for [**1H**] and at −0.74 V vs Fc/Fc^+ for [**2H**] (ΔE_p =

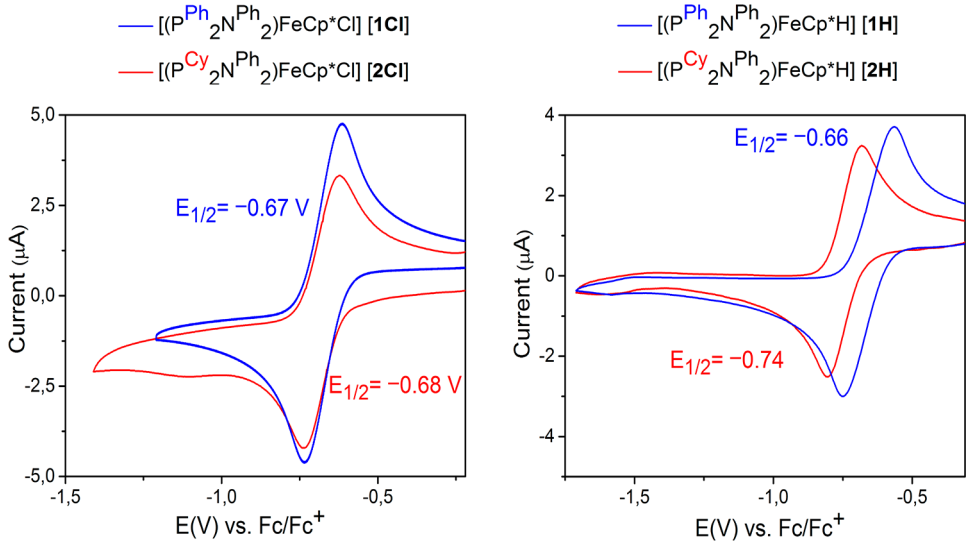

Figure 6. Cyclic voltammograms of chlorido (left) and hydrido (right) compounds in fluorobenzene (1 mmol L^{-1}) recorded at a scan rate of 100 mV/s with NBu_4PF_6 (0.2 M) as the supporting electrolyte.

DOI: 10.1021/acs.inorgchem.5b00911
Inorg. Chem. 2015, 54, 6928−6937

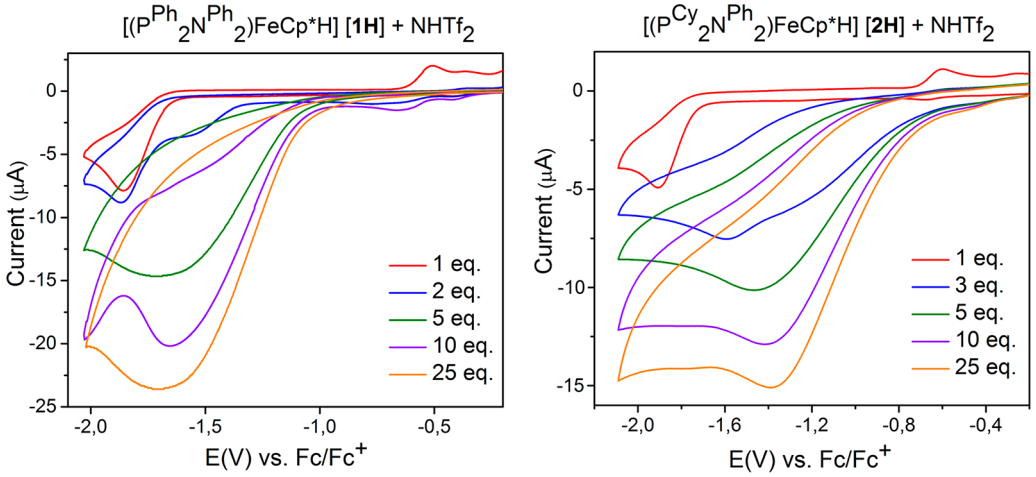

Figure 7. Cyclic voltammograms of [**1H**] and [**2H**] in fluorobenzene in the presence of various amounts of [$NHTf_2$] recorded at a scan rate of 100 mV/s with NBu_4PF_6 (0.2 M) as the supporting electrolyte.

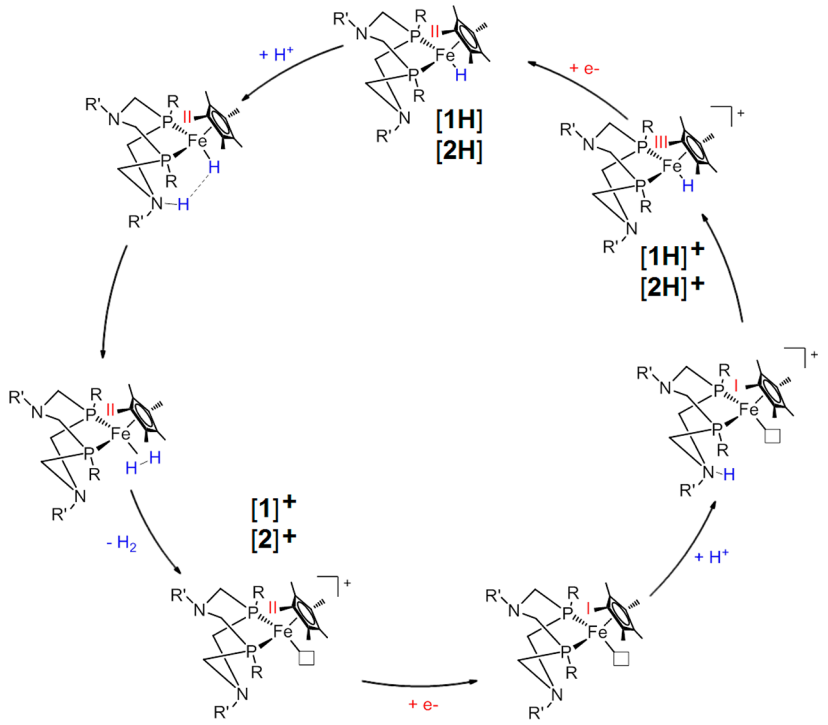

Figure 8. Proposed catalytic cycle for hydrogen production based on the (inverse) catalytic cycle reported by Liu et al.[18] In this work, by choosing a less basic amine in the second coordination sphere and a stronger σ-donating ligand in the first coordination sphere (as compared to that in Liu et al.), it was possible to reverse the catalytic reaction toward hydrogen production in cyclic voltammetry. In the case of Liu et al. (with a different design of ligands), the catalytic cycle was in the reverse direction and thereby resulted in oxidation of H_2.

110 mV, $i_{pa}/i_{pc} \approx 1$).[30] The products of the one-electron oxidation are [Fe(III)−H]$^+$ species [**1H**]$^+$ and [**2H**]$^+$. Fe(III)−H intermediates were proposed by Liu et al. in the catalytic cycle for hydrogen splitting.[17,18] However, in that case, an irreversible redox behavior of the iron hydride compounds [$(P^{Ph}N^{Bn})_2$FeCpH] and [$(P^{tBu}N^{Bn})_2FeCp^{C_6F_5}H$] was reported due to intra- and intermolecular proton transfers.[17,18] Darmon et al. reported on reversible Fe(II)/Fe(III) redox couples for hydride compounds [$(P^RN^{R'}P^R)FeCp^XH$] that contain acyclic diphosphine ligands and therefore larger phosphorus−metal−phosphorus bite angles.[31]

The reversible oxidation observed for [**1H**] and [**2H**] in the present work is enabled by two major changes: (i) the strong σ-electron donor Cp*$^-$ ligand provides sufficient electron density at the metal center such that the oxidation to Fe(III) does not make the hydride very acidic and (ii) the basicity of the pendant amines is crucial: the benzyl-substituted amines in the iron compounds reported by Liu et al. are strongly basic, thus supporting the deprotonation of the oxidized hydride, whereas phenyl-substituted amines in [**1H**] and [**2H**] are weakly basic. The difference in the basicity can be roughly estimated from the pK_B values of the corresponding primary amines benzylamine ($pK_B^{H_2O}$ = 4.66)[32] and aniline ($pK_B^{H_2O}$ = 9.4).[33]

Cyclic voltammograms of [**1H**] and [**2H**] in fluorobenzene solutions titrated with increasing amounts of the bases DBU (1,8-diaza-bicyclo[5.4.0]undec-7-ene) or NEt_3 under a H_2

DOI: 10.1021/acs.inorgchem.5b00911
Inorg. Chem. 2015, 54, 6928−6937

atmosphere did not exhibit enhanced current; thus, it is concluded that [**1H**] and [**2H**] are not active in H_2 oxidation. This is in contrast to the electrocatalytic activity observed by Liu et al. for the complex $[(P^{tBu}N^{Bn})_2FeCp^{C_6F_5}H]$.[18] However, upon addition of increasing amounts of trifluoromethanesulfonimide acid (up to 25 equiv), $(CF_3SO_2)_2NH$, $[NHTf_2]$ (pK_a^{MeCN} = 1.0),[34] cyclic voltammograms displayed increased cathodic current, indicating electrocatalytic proton reduction (Figure 7). After addition of 1 equiv of acid, the reversible redox wave vanishes for both [**1H**] and [**2H**], and a new irreversible wave appears at negative potential values (E_{pc} = −1.86 V vs Fc/Fc^+ for [**1H**] and E_{pc} = −1.90 V vs Fc/Fc^+ for [**2H**]). These waves correspond to the reduction of the formed $[\mathbf{1}]^+$ and $[\mathbf{2}]^+$ species formed after hydride protonation upon hydrogen release (see also Figure 8). They shift to less negative potentials upon further addition of acid with increased current. Bulk electrolysis experiments could not be performed since after a few minutes a black deposit was observed on the working glassy carbon electrode and the electric charge flow dropped. These observations indicate decomposition of the catalyst under these strongly acidic conditions, which has also been observed for other model complexes.[35] Addition of the weaker acid CF_3CO_2H (pK_a^{MeCN} = 12.65)[34] did not lead to catalytic current enhancement. The reason for this is that the anion $CF_3CO_2^-$ blocks the free coordination site of iron after hydride protonation and consecutive hydrogen release. The molecular structure of the corresponding product [**2**CF_3CO_2], derived from single crystal X-ray analysis, is shown in Figure S9.

DISCUSSION

The aim of this work is to develop a better understanding of the electronic properties of possible catalytic intermediates in hydrogen conversion electrocatalysis with particular emphasis on the hydride species. In efficient electrocatalysts of the type $[HNi(P^R_2N^R_2)_2][BF_4]$, thermodynamic properties of the Ni−H bond have been investigated by the DuBois group.[36] Monoiron electrocatalysts are a rather new and promising class of catalysts for hydrogen conversion[14−19] and therefore investigation of isolated intermediates with well-defined molecular iron hydrides is of particular interest.

Our results demonstrate that the iron−hydride compounds $[(P^R_2N^{Ph}_2)FeCp^*H]$ [**1H**] (for R = Ph) and [**2H**] (for R = Cy) have significant covalent bonding character as compared to that of chlorido compounds [**1Cl**] and [**2Cl**]. This is clearly shown by X-ray crystallography, ^{57}Fe Mössbauer, electronic absorption, and FTIR spectroscopy. As a consequence of the high covalency of the Fe−H bond, the electronic properties are strongly affected by the variation of the donor ability of the diphosphine ligand.

With a single 1s valence orbital and absent core electron density, the chemistry of hydrogen may be expected to be rather simple. Nevertheless, the dichotomy of transition metal hydrides is remarkable, as they may have acidic or basic character or even act as hydrogen atom ($H^\bullet$) transfer reagents, depending on the electronic nature of the metal center.[20e,37,38] An Fe−H bond is polarized as $Fe^{\delta+}-H^{\delta-}$ because hydrogen is more electronegative than iron. However, iron hydrido complexes impart much less negative charge to the hydride than that in early transition metal hydride complexes.[39] The reactivity of iron hydrides is, therefore, by trend more protonic than hydridic. Indeed, no typical hydridic reactivity was observed for compounds of the type $[(P^R_2N^{Ph}_2)FeCp^{R'}H]$ since they do not react with water.[17] The acidity of the Fe−H bond directly depends on the oxidation state of iron but also, less intuitively, on the π-back bonding abilities of the ligands.[39] The preparation of $[H_2Fe(CO)_4]$ by Hieber et al. in 1931 was a breakthrough in the field of inorganic chemistry.[40] The compound was later shown to be acidic ($pK_1^{H_2O}$ = 4.4 and $pK_2^{H_2O} \approx 14$),[41] with the corresponding deprotonated anions stabilized by strong π-backbonding of the CO ligands. Keeping this in mind, we can assume the acidity of compounds of the type $[(P^R_2N^{Ph}_2)FeCp^{R'}H]$ to be much lower since the phosphine and Cp-derived ligands are only weakly π-backbonding. Furthermore, we can also expect that the hydrido compound $[(P^{tBu}_2N^{Bn}_2)FeCp^{C_6F_5}H]$ reported by Liu et al. has a more protonic (or less hydridic) hydride than compounds [**1H**] and [**2H**]: the electron-withdrawing group C_6F_5 makes the π^*-orbitals of the Cp ring more accessible for π-backbonding, whereas the σ-electron-donating methyl groups on the Cp* ligand have the opposite effect. Thus, hydride compounds of the type $[(P^R_2N^{Ph}_2)FeCp^{R'}H]$ can be fine-tuned to have more or less protonic character.

Proton reduction catalysis by [**1H**] and [**2H**] using $[NHTf_2]$ as a proton source could be shown only in cyclic voltammetry. Bulk electrolysis could not be performed under turnover conditions because of stability problems in such a strongly acidic environment. A weaker acid could not be used, since the free coordination site was blocked by the strongly coordinating counteranion. Steric bulk is presumably needed here for protection of the reactive site.[17] Assuming that catalytic hydrogen production by $[(P^R_2N^{Ph}_2)FeCp^*H]$ proceeds through the same catalytic cycle as that proposed by Liu et al. for hydrogen uptake catalyzed by $[(P^{tBu}_2N^{Bn}_2)FeCp^{C_6F_5}H]$, both Fe(II)−H and Fe(III)−H species are catalytic intermediates.[18] Liu et al. observed only irreversible oxidation of the Fe(II) hydride $[(P^{tBu}_2N^{Bn}_2)FeCp^{C_6F_5}H]$ for reasons discussed above and because of the strongly basic amine functions nearby that deprotonate the formed protonic Fe(III)−H species. Using the strong σ-donor ligand Cp^{*-} and a less basic amine in the second coordination sphere of iron leads to a reversible Fe(II)−H/Fe(III)−H oxidation and the reversion of the catalytic direction to hydrogen production (see Figure 8 for the proposed catalytic cycle).

Chloro compounds $[(P^R_2N^{Ph}_2)FeCp^*Cl]$ are significantly less covalent, as discussed earlier in the text, and are comparable to cationic species $[(P^R_2N^{Ph}_2)FeCp^*]^+$ involved in the cycle. The electronic structures of [**1Cl**] and [**2Cl**] were found to be very similar in the Fe(II) state. From our results, we can therefore deduce that changes of the donor ability of the ligands have a more significant impact on the hydride-containing intermediates than on those with chloride. This may contribute to our understanding of mechanistic aspects of catalytic processes involving iron hydride intermediates.

Both [NiFe] and [FeFe] hydrogenases are bidirectional enzymes, thus showing that hydrogen splitting and release are nearly thermodynamically neutral and kinetically accessible.[42,43] However, only a few nickel-based homogeneous catalysts were shown to be functional in both directions.[44,45] The example of hydrogen splitting complexes reported by Liu et al. and the compounds with reversed reactivity reported in this work demonstrates that this goal can, in principle, also be achieved for monoiron catalysts. Rational design of the ligands is needed to reverse the catalytic direction by fine tuning the electronic structure of the metal complexes.

DOI: 10.1021/acs.inorgchem.5b00911
Inorg. Chem. 2015, 54, 6928−6937

SUMMARY AND CONCLUSIONS

On the basis of the idea that functional [FeFe] hydrogenase models require only the distal iron site, a series of mononuclear $[(P^{R}_{2}N^{Ph}_{2})FeCp^{*}X]$ compounds with R = phenyl/cyclohexyl and X = Cl/H and incorporated pendant amine bases in the second coordination sphere has been synthesized and characterized. Molecular structures of complexes [**2Cl**], [**1H**], and [**2H**] reveal the typical piano-stool geometry around the iron. All four complexes are diamagnetic due to the low-spin state of the Fe(II) centers. Spectroscopic studies using FTIR, electronic absorption, and ^{57}Fe Mössbauer spectroscopy as well as electrochemical results clearly demonstrate that the electronic properties of the hydride compounds are very sensitive to the change of the phosphine substituent, whereas those of the chlorido compounds are less sensitive at the Fe(III) state and are not sensitive at all in the Fe(II) state. This tendency is due to the higher degree of covalency of the hydride complexes. Since hydride intermediates are discussed and proposed in most catalytic cycles, this result positions hydride complexes as good starting points for the rational design of electrocatalysts.

The tendency for electrocatalytic proton reduction of hydride complexes [**1H**] and [**2H**] has been confirmed by enhanced catalytic currents observed in cyclic voltammetry upon addition of the strong acid trifluoromethanesulfonimide [$NHTf_2$]. Keeping in mind that the related complex $[(P^{tBu}N^{Bn})_2FeCp^{C_6F_5}H]$ was reported by Liu et al. to be an electrocatalyst for hydrogen splitting, our results show that the catalytic direction of these monoiron complexes can be reversed. Thus, the prospect of bidirectional iron-based electrocatalysts for hydrogen conversion is a challenging but achievable goal for future research. This type of monoiron compounds allows for selective modifications of both the phosphine and Cp-derived ligands, which makes them good candidates for further investigations in this endeavor.

EXPERIMENTAL SECTION

Materials. All reactions were carried out under an inert atmosphere of argon using standard Schlenk techniques or a dry argon glovebox (MBraun LabMaster130). The solvents used for chemical reactions were purified by the MBraun MB-SPS-800-Auto solvent purification system. C_6D_6 used for NMR spectroscopy was deoxygenated by three freeze−pump−thaw cycles and stored over molecular sieves in the glovebox. The supporting electrolyte, NBu_4PF_6, used for electrochemistry was purchased from Sigma-Aldrich and dried overnight at 100 °C under vacuum before use. Fluorobenzene used for electrochemistry was HPLC-grade and stabilizer-free, dried over CaH_2, and distilled under argon. The cyclic 1,5-diphospha-3,7-diazacyclooctane ligands ($P^{R}_{2}N^{Ph}_{2}$) were prepared according to literature procedures.[46]

Elemental analysis was performed on an Elementar Vario CHN analyzer.

Spectroscopy. FTIR spectra were recorded at room temperature on a PerkinElmer 2000 NIR FT-Raman spectrometer. For measurements in solution, a KBr cell with a 0.5 mm pathway was used. Measurements in the solid state were carried out in KBr pellets (3 mg of sample in 300 mg of KBr).

NMR spectra were recorded at room temperature using a Bruker DRX 400 spectrometer operating at 400.13 MHz for ^{1}H, 161.98 Hz for ^{31}P, and 100.61 MHz for ^{13}C measurements. Solvent peaks are used as internal references relative to Me_4Si for ^{1}H and ^{13}C chemical shifts (listed in ppm). NMR samples were prepared in the glovebox using J. Young NMR tubes.

Absorption spectra were obtained using a diode-array UV/vis spectrometer (HP 8453). Absorption spectra of samples prepared in an anaerobic chamber were measured in 1 cm pathlength cuvettes sealed with a silicon stopper to retain anaerobic conditions, and spectra were measured quickly (<2 min) after removing from the anaerobic chamber to avoid decomposition. No changes in the absorption spectra were observed over the time scale of these measurements. Averages of three dilutions were considered to obtain accurate extinction coefficients by considering only points within the linear range of the instrument (0.005−1 AU).

Mössbauer Spectroscopy. Mössbauer spectra were recorded on a conventional spectrometer with alternating constant acceleration of the γ-source. The minimum experimental line width was 0.24 mm/s (full width at half-height). The sample temperature was maintained constant in an Oxford Instruments Variox or in an Oxford Instruments Mössbauer-Spectromag. The latter is a split-pair superconducting magnet system for applied fields up to 8 T where the temperature of the sample can be varied in the range 1.5−250 K. The field at the sample is perpendicular to the γ-beam. The ^{57}Co/Rh source (1.8 GBq) was positioned at room temperature inside the gap of the magnet system at a zero-field position by using a re-entrant bore. Isomer shifts are quoted relative to iron metal at 300 K. Magnetic Mössbauer spectra were simulated with the program MX (by E.B.), which calculates magnetically perturbed spectra of diamagnetic sample using the usual nuclear Hamiltonian.[24]

Electrochemistry. All electrochemical measurements were carried out under an argon atmosphere at room temperature using an EG&G PAR 273A instrument. All solutions contained the supporting electrolyte, NBu_4PF_6 (0.2 M in fluorobenzene). For cyclic voltammetry, a standard three-electrode configuration was used consisting of glassy carbon (d = 2 mm) working and counter-electrodes and a Ag wire placed in an $AgNO_3$ (0.01 M in MeCN)/NBu_4PF_6 (0.2 M in MeCN) solution as a pseudoreference electrode. The system was systematically calibrated against ferrocene after each experiment, and all potentials are therefore given vs the Fc/Fc^{+} redox potential. Additions of [$NHTf_2$] were made by syringe as a 2 mol L^{-1} solution in fluorobenzene. After each addition of acid, the cyclic voltammogram was recorded immediately after a few seconds of stirring and once again after additional stirring for approximately 2 min. No significant changes were observed.

Crystal Structure Analysis. Single crystals of [**1H**], [**2H**], and [**2Cl**] were mounted on a Bruker-AXS Kappa Mach3 APEX-II diffractometer equipped with an Incoatec Helios mirror monochromator (Mo Kα λ = 0.71073 Å) and a nitrogen cold stream adjusted to 100 K. Data were integrated and averaged with the program SAINT.[47] Final cell constants were obtained from least-squares fits of all measured reflections. An empirical absorption correction was performed using the Gaussian procedure embedded in SADABS.[48] The structures were readily solved by Patterson methods and subsequent difference Fourier techniques. The Siemens SHELXTL software package was used for solution and artwork of the structures, and SHELXL was used for the refinement.[49,50] All non-hydrogen atoms were anisotropically refined. Hydrogen atoms bound to carbon were placed at calculated positions and refined as riding atoms with isotropic displacement parameters.

Computational Methods. All calculations reported in this article were performed using the ORCA program package.[51,52] Geometry optimizations were carried out at the DFT level using the BP86 GGA functional in conjunction with the RI approximation.[53] Initial atomic coordinates were taken from single-crystal X-ray diffraction experiments for [**1H**], [**2H**], and [**2Cl**]. The starting geometry of [**1Cl**] was derived from the [**1H**] crystal structural data via manual H/Cl substitution. Stationary points were confirmed to be minima by the absence of imaginary frequencies. Details for the computation of the Mössbauer parameters are given in the Supporting Information.

Synthetic Procedures. *Synthesis of [($P^{Ph}_{2}N^{Ph}_{2}$)FeCp*Cl] [**1Cl**].* A suspension of Cp*Li (28 mg, 0.20 mmol) and $FeCl_2(thf)_{1.5}$ (47 mg, 0.2 mmol) in THF (3 mL) was stirred at −40 °C for 5 min until a green solution was obtained.[23] Ligand $P^{Ph}_{2}N^{Ph}_{2}$ (91 mg, 0.2 mmol) was added as a solid, and the solution immediately turned dark brown. The solution was allowed to warm to room temperature and was stirred for 10−15 min. n-Hexane (1 mL) was added, and a white precipitate (LiCl) was filtered off. The filtrate was overlaid by n-hexane

DOI: 10.1021/acs.inorgchem.5b00911
Inorg. Chem. 2015, 54, 6928−6937

(6 mL) and stored at −40 °C. The product was isolated as black crystals and dried under reduced pressure (87 mg, 65%). ^{1}H NMR (THF-d_8, 400 MHz, 300 K): δ 8.06 (m, 4H, Ar), 7.58−7.48 (m, 6H, Ar), 7.34−7.24 (m, 4H, Ar), 7.02 (m, 2H, Ar), 6.85−6.65 (m, 4H, Ar), 4.57 (d, 2H, $^{2}J_{HH}$ = 13 Hz, CH_2), 4.10 (d, 2H, $^{2}J_{HH}$ = 12 Hz, CH_2), 3.71 (d, 2H, $^{2}J_{HH}$ = 13 Hz, CH_2), 4.57 (dt, 2H, $^{2}J_{HH}$ = 12 Hz, $^{2}J_{PH}$ = 7 Hz, CH_2), 1.15 (s, 15H, CH_3). $^{13}C\{^{1}H\}$ NMR (THF-d_8, 100 MHz, 300 K): δ 153.6 (C_q), 139.7 (C_q), 131.4 (CH), 130.2 (CH), 129.8 (CH), 129.4 (CH), 120.8 (CH), 120.0 (CH), 118.2 (CH), 116.1 (CH), 86.0 (C_q), 52.1 (CH_2), 46.4 (CH_2), 10.1 (CH_3). $^{31}P\{^{1}H\}$ NMR (THF-d_8, 162 MHz, 300 K): δ 51.0. ^{57}Fe Mössbauer (80 K, 0 T): δ = 0.46 mm/s, ΔE_Q = 2.23 mm/s. Anal. Calcd for $C_{38}H_{43}FeClN_2P_2$: C, 67.02; H, 6.36; N, 4.11. Found: C, 67.19; H, 6.68; N, 3.96. UV−vis (THF): λ (nm), ε (cm^{-1} mM^{-1}): 403 (0.99), 499 (0.67), 585 (0.35).

*Synthesis of [($P^{Cy}_2N^{Ph}_2$)FeCp*Cl] [**2Cl**] Was Performed in Analogy to That for [**1Cl**].* The product was isolated as a dark purple solid in 68−79% yield. X-ray suitable crystals of [**2Cl**] were grown by the overlaying technique from THF and *n*-hexane at −40 °C. ^{1}H NMR (THF-d_8, 400 MHz, 300 K): δ 7.15 (m, 4H, Ar), 7.06 (d, 2H, Ar), 6.95 (d, 2H, Ar), 6.74 (t, 2H, Ar), 3.88 (d, 2H, $^{2}J_{HH}$ = 13 Hz, CH_2), 3.50 (d, 2H, $^{2}J_{HH}$ = 11 Hz, CH_2), 3.02 (br d, 2H, CH_2), 2.88 (br t, 2H, CH_2), 2.69 (br d, 2H, CH_2), 2.61 (br m, 2H, CH_2), 2.22 (d, 2H, $^{2}J_{HH}$ = 12 Hz, CH_2), 1.98 (d, 2H, $^{2}J_{HH}$ = 13 Hz, CH_2), 1.90 (d, 2H, $^{2}J_{HH}$ = 12 Hz, CH_2), 1.84−1.67 (overlaid with THF signal, 4H, CH_2), 1.64−1.29 (m, 21H, CH_3 and CH_2), 1.08 (m, 4H, CH_2). $^{13}C\{^{1}H\}$ NMR (THF-d_8, 100 MHz, 300 K): δ 146.1 (C_q), 129.7 (CH), 120.6 (CH), 118.4 (CH), 116.2 (CH), 83.8 (C_q), 68.1 (CH_2), 29.1 (CH_2), 28.5 (CH_2), 28.2 (CH_2), 28.0 (CH_2), 27.4 (CH_2), 10.7 (CH_3). $^{31}P\{^{1}H\}$ NMR (THF-d_8, 162 MHz, 300 K): δ 53.2. ^{57}Fe Mössbauer (80 K, 0 T): δ = 0.46 mm/s, ΔE_Q = 2.14 mm/s. Anal. Calcd for $C_{38}H_{55}FeClN_2P_2$: C, 65.85; H, 8.00; N, 4.04. Found: C, 65.32; H, 8.11; N, 4.12. UV−vis (THF): λ (nm), ε (cm^{-1} mM^{-1}): 398 (0.33), 485 (0.88), 575 (0.29).

*Synthesis of [($P^{Ph}_2N^{Ph}_2$)FeCp*H] [**1H**].* To a THF solution of [**1Cl**] prepared *in situ* as described above was added 2.2 equiv of $LiAlH_4$ at −40 °C. The suspension was allowed to warm to room temperature, and the color changed from brown to orange. After stirring the reaction mixture for 15 min at room temperature, the solvent was removed under reduced pressure and the residue was extracted with *n*-hexane. Unreacted $LiAlH_4$ was filtered off, and *n*-hexane was removed under reduced pressure. The product was isolated as an orange solid in 65−71% yield. The same procedure can be used for the synthesis of [**1H**] starting from the isolated compound [**1Cl**] in higher yields (78−92%). X-ray suitable crystals of [**1H**] were grown from a saturated solution in *n*-hexane at −40 °C. ^{1}H NMR (C_6D_6, 400 MHz, 300 K): δ 7.63−7.56 (m, 4H, Ar), 7.35−7.28 (m, 2H, Ar), 7.25−7.18 (m, 6H, Ar), 7.00−6.90 (m, 3H, Ar), 6.69 (m, 1H, Ar), 6.50 (m, 2H, Ar), 4.10 (d, 2H, $^{2}J_{HH}$ = 13 Hz, CH_2), 3.64 (m, 2H, CH_2), 3.40 (m, 2H, CH_2), 3.12 (d, 2H, $^{2}J_{HH}$ = 13 Hz, CH_2), 1.55 (s, 15H, CH_3), −15.8 (t, 1H, $^{2}J_{PH}$ = 60 Hz, FeH). $^{13}C\{^{1}H\}$ NMR (C_6D_6, 100 MHz, 300 K): δ 154.7 (C_q), 153.4 (C_q), 138.7 (C_q), 130.5 (CH), 129.6 (CH), 129.3 (CH), 128.7 (CH), 128.6 (CH), 119.9 (CH), 119.7 (CH), 117.1 (CH), 86.4 (C_q), 61.0 (CH_2), 48.1 (CH_2), 11.7 (CH_3). $^{31}P\{^{1}H\}$ NMR (C_6D_6, 162 MHz, 300 K): δ 67.1. ^{57}Fe Mössbauer (80 K, 0 T): δ = 0.20 mm/s, ΔE_Q = 2.11 mm/s. Anal. Calcd for $C_{38}H_{44}FeN_2P_2$: C, 70.59; H, 6.86; N, 4.33. Found: C, 70.45; H, 7.11; N, 4.18. UV−vis (THF): λ (nm), ε (cm^{-1} mM^{-1}): 388 (1.74). FTIR (KBr) = 1808 cm^{-1} (FeH).

*Synthesis of [($P^{Cy}_2N^{Ph}_2$)FeCp*H] [**2H**] Was Performed in Analogy to That for [**1H**].* The product was isolated as a yellow solid in 65% yield from *in situ* prepared [**2Cl**] and in 81−88% yield starting from isolated [**2Cl**]. X-ray suitable crystals of [**2H**] were grown from a saturated solution in *n*-hexane at −40 °C. ^{1}H NMR (C_6D_6, 400 MHz, 300 K): δ 7.26 (m, 2H, Ar), 7.14 (m, 4H, Ar), 6.89−6.79 (m, 4H, Ar), 3.83 (quintet, 2H, $^{3}J_{HH}$ = 7 Hz, CH), 3.69 (d, 2H, $^{2}J_{HH}$ = 13 Hz, NCH_2P), 2.88 (d, 2H, $^{2}J_{HH}$ = 13 Hz, NCH_2P), 2.49 (d, 2H, $^{2}J_{HH}$ = 13 Hz, NCH_2P), 2.40 (d, 2H, $^{2}J_{HH}$ = 13 Hz, NCH_2P), 2.24 (m, 2H, CH_2), 1.93 (s, 15H, CH_3), 1.85−1.64 (m, 8H, CH_2), 1.37−1.20 (m, 6H, CH_2), 1.09−0.90 (m, 4H, CH_2), −16.6 (t, 1H, $^{2}J_{PH}$ = 62 Hz, FeH). $^{13}C\{^{1}H\}$ NMR (C_6D_6, 100 MHz, 300 K): δ 155.3 (C_q), 154.3 (C_q), 129.5 (CH), 128.3 (CH), 120.9 (CH), 119.0 (CH), 118.6 (CH), 115.8 (CH), 85.3 (C_q), 55.1 (CH_2), 47.3 (CH_2), 28.6 (CH_2), 28.0 (CH_2), 27.8 (CH_2), 27.3 (CH_2), 26.9 (CH_2), 12.3 (CH_3). $^{31}P\{^{1}H\}$ NMR (C_6D_6, 162 MHz, 300 K): δ 69.3. ^{57}Fe Mössbauer (80 K, 0 T): δ = 0.23 mm/s, ΔE_Q = 2.23 mm/s. Anal. Calcd for $C_{38}H_{56}FeN_2P_2$: C, 69.29; H, 8.57; N, 4.25. Found: C, 69.44; H, 8.17; N, 4.43. UV−vis (THF): λ (nm), ε (cm^{-1} mM^{-1}): 407 (1.13). FTIR (KBr) = 1783 cm^{-1} (FeH).

■ ASSOCIATED CONTENT

Ⓢ Supporting Information

Crystallographic data and NMR, Mössbauer, FTIR, and absorption spectra. Crystallographic data are also provided in CIF format. The Supporting Information is available free of charge on the ACS Publications website at DOI: 10.1021/acs.inorgchem.5b00911.

■ AUTHOR INFORMATION

Corresponding Authors

*(O.F.E.) E-mail: oezlen-ferruh.erdem@cec.mpg.de.
*(W.L.) E-mail: wolfgang.lubitz@cec.mpg.de.

Notes

The authors declare no competing financial interest.

■ ACKNOWLEDGMENTS

This work was supported by the Max Planck Society. We also thank the Fonds der Chemischen Industrie for the Doctoral Kekulé Fellowship (K.W.). Inge Heise is gratefully acknowledged for the synthesis of the phosphine ligands. We thank Bernd Mienert for help with the Mössbauer measurements. Julian Jacobs is gratefully acknowledged for UV/vis spectra measurements.

■ REFERENCES

(1) (a) Vignais, P. M.; Billoud, B. *Chem. Rev.* **2007**, *107*, 4206−4272. (b) Frey, M. *ChemBioChem* **2002**, *3*, 153−160. (c) Lubitz, W.; Reijerse, E.; van Gastel, M. *Chem. Rev.* **2007**, *107*, 4331−4365. (d) Lubitz, W.; Ogata, H.; Rüdiger, O.; Reijerse, E. *Chem. Rev.* **2014**, *114*, 4081−4148.

(2) Nicolet, Y.; de Lacey, A. L.; Vernède, X.; Fernandez, V. M.; Hatchikian, E. C.; Fontecilla-Camps, J. C. *J. Am. Chem. Soc.* **2001**, *123*, 1596−1601.

(3) Silakov, A.; Wenk, B.; Reijerse, E.; Lubitz, W. *Phys. Chem. Chem. Phys.* **2009**, *11*, 6592−6599.

(4) Berggren, G.; Adamska, A.; Lambertz, C.; Simmons, T. R.; Esselborn, J.; Atta, M.; Gambarelli, S.; Mouesca, J. M.; Reijerse, E.; Lubitz, W.; Happe, T.; Artero, V.; Fontecave, M. *Nature* **2013**, *499*, 66−69.

(5) Bruschi, M.; Greco, C.; Kaukonen, M.; Fantucci, P.; Ryde, U.; De Gioia, L. *Angew. Chem., Int. Ed.* **2009**, *48*, 3503−3506.

(6) Siegbahn, P. E. M.; Tye, J. W.; Hall, M. B. *Chem. Rev.* **2007**, *107*, 4414−4435.

(7) Adamska, A.; Silakov, A.; Lambertz, C.; Rüdiger, O.; Happe, T.; Reijerse, E.; Lubitz, W. *Angew. Chem., Int. Ed.* **2012**, *51*, 11458−11462.

(8) Artero, V.; Fontecave, M. *Coord. Chem. Rev.* **2005**, *249*, 1518−1535.

(9) Wang, M.; Chen, L.; Sun, L. *Energy Environ. Sci.* **2012**, *5*, 6763−6778.

(10) Bullock, M. R. *Science* **2013**, *342*, 1080−1083.

(11) (a) Darensbourg, M. Y.; Lyon, E. J.; Smee, J. J. *Coord. Chem. Rev.* **2000**, *206−207*, 533−561. (b) Tard, C.; Pickett, C. J. *Chem. Rev.* **2009**, *109*, 2245−2274. (c) Gloaguen, F.; Rauchfuss, T. B. *Chem. Soc. Rev.* **2009**, *38*, 100−108. (d) Capon, J. F.; Gloaguen, F.; Pétillon, F. Y.; Schollhammer, P.; Talarmin, J. *Coord. Chem. Rev.* **2009**, *253*, 1476−1494. (e) Simmons, T. R.; Berggren, G.; Bacchi, M.; Fontecave, M.; Artero, V. *Coord. Chem. Rev.* **2014**, *270−271*, 127−150. (f) Karnahl, M.; Tschierlei, S.; Erdem, Ö. F.; Pullen, S.; Santoni, M. P.; Reijerse, E.

DOI: 10.1021/acs.inorgchem.5b00911
Inorg. Chem. 2015, 54, 6928−6937

J.; Lubitz, W.; Ott, S. *Dalton Trans.* **2012**, *41*, 12468−12477. (g) Erdem, Ö. F.; Schwartz, L.; Stein, M.; Silakov, A.; Kaur-Ghumaan, S.; Huang, P.; Ott, S.; Reijerse, E. J.; Lubitz, W. *Angew. Chem., Int. Ed.* **2011**, *50*, 1439−1443. (h) Justice, A. K.; Nilges, M. J.; Rauchfuss, T. B.; Wilson, S. R.; De Gioia, L.; Zampella, G. *J. Am. Chem. Soc.* **2008**, *130*, 5293−5301. (i) Erdem, Ö. F.; Stein, M.; Kaur-Ghumaan, S.; Reijerse, E. J.; Ott, S.; Lubitz, W. *Chem.—Eur. J.* **2013**, *19*, 14566−14572.

(12) (a) Ezzaher, S.; Capon, J. F.; Gloaguen, F.; Pétillon, F. Y.; Schollhammer, P.; Talarmin, J.; Pichon, R.; Kervarec, N. *Inorg. Chem.* **2007**, *46*, 3426−3428. (b) Barton, B. E.; Rauchfuss, T. B. *Inorg. Chem.* **2008**, *47*, 2261−2263. (c) Wright, J. A.; Pickett, C. J. *Chem. Commun.* **2009**, *38*, 5719−5721. (d) Jablonskyte, A.; Wright, J. A.; Pickett, C. J. *Dalton Trans.* **2010**, *39*, 3026−3034. (e) Carroll, M. E.; Barton, B. E.; Rauchfuss, T. B.; Carroll, P. J. *J. Am. Chem. Soc.* **2012**, *134*, 18843−18852. (f) Zaffaroni, R.; Rauchfuss, T. B.; Gray, D. L.; De Gioia, L.; Zampella, G. *J. Am. Chem. Soc.* **2012**, *134*, 19260−19269.

(13) Felton, G. A. N.; Vannucci, A. K.; Okumura, N.; Lockett, L. T.; Evans, D. H.; Glass, R. S.; Lichtenberger, D. L. *Organometallics* **2008**, *27*, 4671−4679.

(14) Kaur-Ghumaan, S.; Schwartz, L.; Lomoth, R.; Stein, M.; Ott, S. *Angew. Chem., Int. Ed.* **2010**, *49*, 8033−8036.

(15) Beyler, M.; Ezzaher, S.; Karnahl, M.; Santoni, M. P.; Lomoth, R.; Ott, S. *Chem. Commun.* **2011**, *47*, 11662−11664.

(16) Orthaber, A.; Karnahl, M.; Tschierlei, S.; Streich, D.; Stein, M.; Ott, S. *Dalton Trans.* **2014**, *43*, 4537−4549.

(17) Liu, T.; Chen, S.; O'Hagan, M. J.; Rakowski DuBois, M.; Bullock, R. M.; DuBois, D. L. *J. Am. Chem. Soc.* **2012**, *134*, 6257−6272.

(18) Liu, T.; DuBois, D. L.; Bullock, R. M. *Nat. Chem.* **2013**, *5*, 228−233.

(19) Liu, T.; Wang, X.; Hoffmann, C.; DuBois, D. L.; Bullock, R. M. *Angew. Chem., Int. Ed.* **2014**, *53*, 5300−5304.

(20) (a) Bolm, C.; Legros, J.; Le Paih, J.; Zani, L. *Chem. Rev.* **2004**, *104*, 6217−6254. (b) Morris, R. H. *Chem. Soc. Rev.* **2009**, *38*, 2282−2291. (c) Nakazawa, H.; Itazaki, M. *Fe−H Complexes in Catalysis*; Springer: Berlin, 2011; pp 27−81. (d) *Iron Catalysis in Organic Chemistry*; Plietker, B., Ed.; Wiley-VCH: Weinheim, Germany, 2008. (e) Bullock, M. R. *Catalysis without Precious Metals*; Wiley-VCH: Weinheim, Germany, 2010.

(21) (a) Bullock, R. M.; Appel, A. M.; Helm, M. L. *Chem. Commun.* **2014**, *50*, 3125−3143. (b) Darmon, J. M.; Kumar, N.; Hulley, E. B.; Weiss, C. J.; Raugei, S.; Bullock, R. M.; Helm, M. L. *Chem. Sci.* **2015**, *6*, 2737−2745.

(22) Weber, K.; Erdem, Ö. F.; Bill, E.; Weyhermüller, T.; Lubitz, W. *Inorg. Chem.* **2014**, *53*, 6329−6337.

(23) Roger, C.; Hamon, P.; Toupet, L.; Rabaa, H.; Saillard, J. Y.; Hamon, J. R.; Lapinte, C. *Organometallics* **1991**, *10*, 1045−1054.

(24) Gütlich, P.; Bill, E.; Trautwein, A. X. *Mössbauer Spectroscopy and Transition Metal Chemistry*; Springer: Heildelberg, 2011.

(25) Nakamoto, K. *Infrared and Raman Spectra of Inorganic and Coordination Compounds*; John Wiley & Sons: Hoboken, NJ, 2008.

(26) Belkova, N. V.; Epstein, L. M.; Filippov, O. A.; Shubina, E. S. *Spectrosc. Prop. Inorg. Organomet. Compd.* **2012**, *43*, 1−28.

(27) Shriver, D. F.; Atkins, P. W.; Langford, C. H. *Inorg. Chem.* **1990**, 192−223.

(28) One-electron oxidized samples were prepared electrochemically by constant potential coulometry at −35 °C in fluorobenzene in a dry argon glovebox. The EPR spectra of $[\mathbf{1Cl}]^+$ and $[\mathbf{2Cl}]^+$ measured at X-band at 10 K (not shown) revealed well-resolved *g*-values of (2.314, 2.066, 2.005) and (2.327, 2.068, 2.001), respectively. This indicates that for these compounds the piano-stool geometry is maintained in frozen solution.

(29) Tilset, M.; Fjeldahl, I.; Hamon, J. R.; Hamon, P.; Toupet, L.; Saillard, J. Y.; Costuas, K.; Haynes, A. *J. Am. Chem. Soc.* **2001**, *123*, 9984−10000.

(30) EPR spectra of one-electron oxidized compounds (prepared as described above), $[\mathbf{1H}]^+$ and $[\mathbf{2H}]^+$, were composed of at least two species for which the *g*-values could not be exclusively identified. Moreover, the H/D exchange for $[\mathbf{1H}]^+$ and $[\mathbf{2H}]^+$ did not lead to any changes in the CW EPR or Q-Band ENDOR spectra at 2 K. This is, presumably, due to decomposition during the time course of coulometric one-electron oxidation in fluorobenzene. Trapping the stable Fe(III)−H species is in progress, but it is outside the scope of this work and will be reported in a separate paper.

(31) Darmon, J. M.; Raugei, S.; Liu, T.; Hulley, E. B.; Weiss, C. J.; Bullock, R. M.; Helm, M. L. *ACS Catal.* **2014**, *4*, 1246−1260.

(32) Hall, H. K. *J. Am. Chem. Soc.* **1957**, *79*, 5441−5444.

(33) Clayden, J.; Greeves, N.; Warren, S.; Wothers, P. *Organic Chemistry*; Oxford University Press: Oxford, 2001; pp 47−79.

(34) Kütt, A.; Rodima, T.; Saame, J.; Raamat, E.; Mäemets, V.; Kaljurand, I.; Koppel, I. A.; Garlyauskayte, R. Y.; Yagupolskii, Y. L.; Yagupolskii, L. M.; Bernhardt, E.; Willner, H.; Leito, I. *J. Org. Chem.* **2011**, *76*, 391−395.

(35) Hsieh, C. H.; Ding, S.; Erdem, Ö. F.; Crouthers, D. J.; Liu, T.; McCrory, C. C. L.; Lubitz, W.; Popescu, C. V.; Reibenspies, J. H.; Hall, M. B.; Darensbourg, M. Y. *Nat. Commun.* **2014**, *5*, 1−8.

(36) (a) Berning, D. E.; Miedaner, A.; Curtis, C. J.; Noll, B. C.; Rakowski DuBois, M. C.; DuBois, D. L. *Organometallics* **2001**, *20*, 1832−1839. (b) Curtis, C. J.; Miedaner, A.; Ciancanelli, R.; Ellis, W. W.; Noll, B. C.; Rakowski DuBois, M.; DuBois, D. L. *Inorg. Chem.* **2002**, *42*, 216−227. (c) Fraze, K.; Wilson, A. D.; Appel, A. M.; Rakowski DuBois, M.; DuBois, D. L. *Organometallics* **2007**, *26*, 3918−3924.

(37) Bullock, R. M. *Comments Inorg. Chem.* **1991**, *12*, 1−33.

(38) Pearson, R. G. *Chem. Rev.* **1985**, *85*, 41−49.

(39) Labinger, J. A.; Komadina, K. H. *J. Organomet. Chem.* **1978**, *155*, C25−C28.

(40) Hieber, W.; Leutert, F. *Naturwissenschaften* **1931**, *19*, 360−361.

(41) Krumholz, P.; Stettiner, H. M. A. *J. Am. Chem. Soc.* **1949**, *71*, 3035−3039.

(42) Vincent, K. A.; Parkin, A.; Armstrong, F. A. *Chem. Rev.* **2007**, *107*, 4366−4413.

(43) Armstrong, F. A.; Belsey, N. A.; Cracknell, J. A.; Goldet, G.; Parkin, A.; Reisner, E.; Vincent, K. A.; Wait, A. F. *Chem. Soc. Rev.* **2009**, *38*, 36−51.

(44) Smith, S. E.; Yang, J. Y.; DuBois, D. L.; Bullock, R. M. *Angew. Chem., Int. Ed.* **2012**, *51*, 3152−3155.

(45) Dutta, A.; Lense, S.; Hou, J.; Engelhard, M. H.; Roberts, J. A. S.; Shaw, W. J. *J. Am. Chem. Soc.* **2013**, *135*, 18490−18496.

(46) Märkl, G.; Jin, G. Y.; Schoerner, C. *Tetrahedron Lett.* **1980**, *21*, 1409−1412.

(47) *SAINT*, version 7.46A; Bruker-AXS Inc.: Madison, WI, 2008.

(48) *SADABS*, version 2009/1; Bruker-AXS Inc.: Madison, WI, 2009.

(49) *SHELXTL*, 2013/2; Bruker AXS Inc.: Madison, WI, 2013.

(50) Sheldrick, G. M. *SHELXL*; University of Göttingen: Göttingen, 2013.

(51) Neese, F. *WIREs Comput. Mol. Sci.* **2012**, *2*, 73−78.

(52) Neese, F. *ORCA—an ab Initio, DFT and Semiempirical Electronic Structure Package*, version 2.9.0; University of Bonn: Bonn, Germany, 2012.

(53) (a) Becke, A. D. *Phys. Rev. A* **1988**, *38*, 3098−3100. (b) Perdew, J. P. *Phys. Rev. B* **1986**, *33*, 8822−8824. (c) Baerends, E. J.; Ellis, D. E.; Ros, P. *Chem. Phys.* **1973**, *2*, 41−51. (d) Dunlap, B. I.; Connolly, J. W. D.; Sabin, J. R. *J. Chem. Phys.* **1979**, *71*, 3396−3403. (e) Vahtras, O.; Almlöf, J.; Feyereisen, M. W. *Chem. Phys. Lett.* **1993**, *213*, 514−518. (f) Neese, F. *J. Comput. Chem.* **2003**, *24*, 1740−1747.

DOI: 10.1021/acs.inorgchem.5b00911
Inorg. Chem. 2015, 54, 6928−6937